BULLETIN OF THE POLISH ACADEMY OF SCIENCES
TECHNICAL SCIENCES, Vol. 62, No. 1, 2014
*DOI: 10.2478/bpasts-2014-0015*

# Basic set of experiments for determination of mechanical properties of sand

A. SAWICKI, J. MIERCZYŃSKI*, and W. ŚWIDZIŃSKI

Institute of Hydro-Engineering, Polish Academy of Sciences, 7 Kościerska St., 80-328 Gdańsk-Oliwa, Poland

**Abstract.** A basic set of experiments for the determination of mechanical properties of sands is described. This includes the determination of basic physical and mechanical properties, as conventionally applied in soil mechanics, as well as some additional experiments, which provide further information on mechanical properties of granular soils. These additional experiments allow for determination of steady state and instability lines, stress-strain relations for isotropic loading and pure shearing, and simple cyclic shearing tests. Unconventional oedometric experiments are also presented. Necessary laboratory equipment is described, which includes a triaxial apparatus equipped with local strain gauges, an oedometer capable of measuring lateral stresses and a simple cyclic shearing apparatus. The above experiments provide additional information on soil's properties, which is useful in studying the following phenomena: pre-failure deformations of sand including cyclic loading compaction, pore-pressure generation and liquefaction, both static and caused by cyclic loadings, the effect of sand initial anisotropy and various instabilities. An important feature of the experiments described is that they make it possible to determine the initial state of sand, defined as either contractive or dilative. Experimental results for the "Gdynia" model sand are shown.

**Key words:** granular soils, mechanical properties, experimental determination.

## 1. Introduction

In granular soils there appear various phenomena which are not observed in other materials, such as dilation, compaction, liquefaction, characteristic instabilities, etc. Such phenomena, as well as other soil properties, like strength and deformability, have been described by a constantly increasing number of various models, more and more complex and difficult to comprehend. Most such models produce "virtual predictions in a computer game environment" [1], or they are such that "no other researcher is able to work with them" [2]. They are even less useful for practicing geotechnical engineers, who need relatively simple and reliable models.

One of the basic difficulties in soil mechanics is that each such model includes a large number of various parameters/constants, which should be determined experimentally, most of them having no physical meaning. The number of such parameters increases as the model becomes more complex in attempting to be more universal. On the other hand, geotechnical engineers have remained traditional, and they develop their own tools, based mainly on empirical knowledge. These two branches, that is, geomechanics and geotechnical engineering, develop almost independently. However, they have some problems in common, and one of them is "a minimal set of parameters" necessary to characterize mechanical properties of granular soils.

The other problem is whether to develop universal models, which describe most phenomena, or to use a set of simple models, each of them describing just a few of those phenomena. An obvious candidate for such a set of models is the limit states theory, which is well elaborated in geotechnical literature, and leads to reasonable predictions of many practical problems, cf. [3, 4]. Various soil mechanics workshops and even schools suggest that many attempts to develop sufficiently general models have not been particularly successful, see [5]. Therefore, it may be a more efficient approach to develop a set of relatively simple models, and to select some basic experiments, on the basis of which necessary parameters could be determined or respective models calibrated.

In this paper, several experiments leading to the determination of various mechanical properties of granular soils are proposed as a basic set, and some useful methods of dealing with experimental data are shown. A particularly efficient method is the one which makes it possible to present various experimentally obtained curves in the form of a single (common) curve. This set of experiments includes standard geotechnical investigations aimed at determining the basic physical and mechanical properties of sand, and some other unconventional experiments performed in the following devices: a triaxial apparatus capable of measuring local strains (both lateral and vertical ones), an oedometer capable of measuring lateral stresses, and a simple cyclic shear apparatus. A set of basic experimental results is presented and discussed in the context of their potential usefulness. This basic set of experimental data makes it possible to calibrate various models which describe the following phenomena: limit states, pre-failure deformations and instabilities, static liquefaction, cyclic loading compaction and liquefaction, etc.

## 2. Standard physical and mechanical properties

All experiments described in this paper were performed on the quartz "Gdynia" sand characterized by the following parameters: median size of grains $D_{50} = 0.565$ mm; uniformity co-

*e-mail: mier@ibwpan.gda.pl

efficient $C_U = 1.66$; specific gravity $G = 2.6545$; maximum and minimum void ratios $e_{\max} = 0.746$ and $e_{\min} = 0.500$, respectively; angles of internal friction for loose and medium dense sand $\phi = 31^\circ$ ($I_D = 0.3$) and $\phi = 34^\circ$ ($I_D = 0.48$). Figure 1 shows the particle size distribution curve for the "Gdynia" sand.

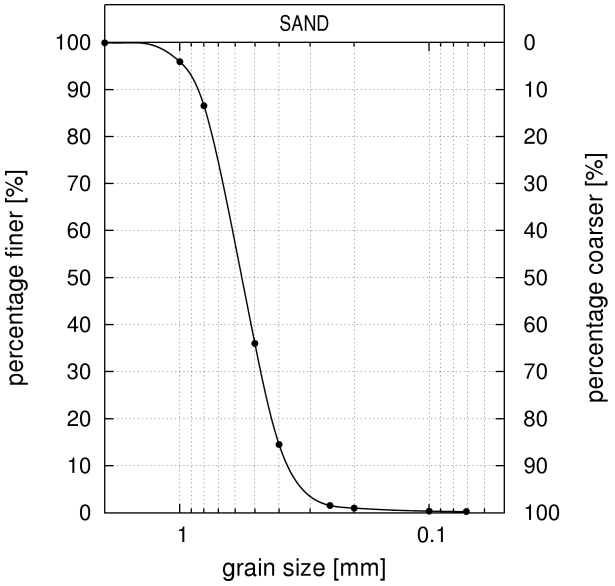


Fig. 1. The particle size distribution curve for the "Gdynia" sand

The angles of internal friction were determined from triaxial compression tests. Specimens were prepared in a membrane-lined moulder by moist tamping (loose specimens) or dry pluviation (dense specimens). Triaxial compression tests were performed in a computer-controlled device manufactured by GDS Instruments, see [6]. The apparatus was equipped with special gauges for the local measurement of vertical and lateral strains.

## 3. Determination of the steady state line

The behaviour of granular soil strongly depends on its initial state. One of the main parameters describing the initial state is the relative density $D_r$, sometimes also designated as the density index $I_D$, which expresses the relationship between the actual void ratio $e$ and the limiting values of this parameter, i.e. $e_{\max}$, $e_{\min}$ [7]. Low values of the relative density correspond to loose sands, higher values to dense sands.

However, a single parameter, such as the relative density, does not provide sufficient information about the initial state of sand, as two samples characterized by the same values of $D_r$ (or $e$) may behave differently, depending on the respective values of the initial mean effective stress $p'$. In order to include these two important parameters in the description of the initial state of sand, the concept of a steady state line has been proposed. This concept is based on steady state soil mechanics, initiated by pioneering works of Castro [8] and Poulos [9], and later developed by others, including Been and Jefferies [10], Been et al. [11], Chu and Leong [12]. Recall that the steady state is defined as a continuous deformation of sand under a constant volume and constant stress.

The steady state line (SSL) is plotted in the $(p', e)$ plane, as shown in Fig. 2, representing the "Gdynia" sand. An initial state of soil is defined by a point in this space. Points lying above SSL represent initially contractive states, whereas points below this line correspond to initially dilative states. Basic differences between the behaviour of initially contractive and dilative sands will be shown in subsequent sections.

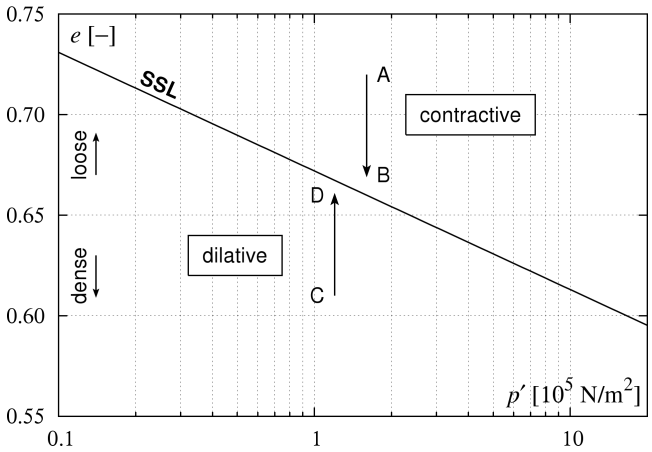


Fig. 2. The steady state line for the "Gdynia" sand

SSL is determined from a set of triaxial tests, performed on saturated sand under both undrained and fully drained conditions, for different initial values of the void ratio and the effective mean stress. Specimens are sheared along the standard geotechnical stress path, i.e. the horizontal stress is kept constant, and the vertical stress increases up to the steady state. Under fully drained conditions, the steady state is achieved at large vertical strains of up to 30%. Under undrained conditions, for initially contractive soils, such a procedure leads to static liquefaction.

After a few experiments, one obtains a set of points in the $(p', e)$ space, which can be approximated by a straight line, i.e. SSL. There are different opinions on the shape of SSL, because for small and large stresses it may deviate from a straight line, or it may even resemble a fuzzy strip rather than a line.

Definition of the initial state of the granular soil in terms of two parameters is of a great importance from the view point of its response under shear load. This problem however has been not addressed neither in classical Polish books such as [13] nor in recent ones with new theoretical approaches such as hypoplasticity, see [14].

## 4. Stress-strain relations for triaxial conditions

**4.1. Introduction.** The triaxial apparatus is the basic piece of equipment in most geotechnical laboratories, see Fig. 3. Recently, such devices have been equipped with additional gauges for the local measurement of both vertical and lateral strains, making it possible to collect a full set of data on the pre-failure response of sands, both drained and undrained,

and consequently to determine stress-strain curves and other geometrical objects, such as the instability line.

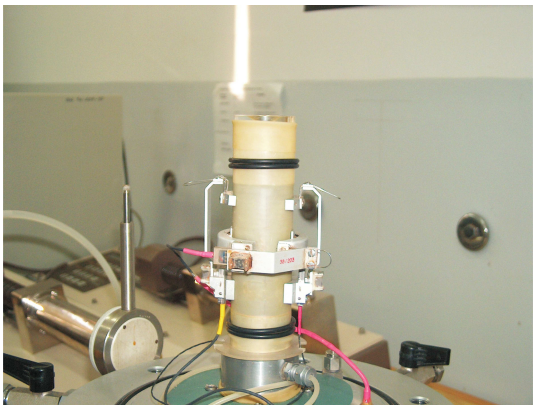

Fig. 3. A soil specimen prepared for investigations in the GDS triaxial apparatus. Strain gauges are installed directly on the specimen

It is proposed that two basic types of experiments are performed: isotropic compression (path 0A in Fig. 4) and pure shearing at the constant mean stress (path ABC in Fig. 4). Here, $q = \sigma_1 - \sigma_3$ is the stress deviator and $p' = (\sigma_1 + 2\sigma_3)/3$ is the mean stress; $\sigma_1$ and $\sigma_3$ are the vertical and horizontal stresses respectively. Both types of experiments should be performed for initially dilative and contractive sands, and they should include loading (paths 0A and ABC) and unloading (paths CBA and A0). Shearing tests (path ABC) should be performed for different values of the constant mean stress – at least three experiments are recommended. During all experiments, both vertical and lateral strains should be recorded. Under undrained conditions, it is necessary to measure the pore pressure.

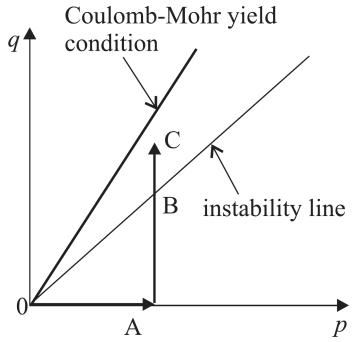


Fig. 4. Basic stress paths for the determination of stress-strain curves

A convenient method of the graphical presentation of experimental data is in terms of the mean effective stress $p'$, the stress deviator $q$, the volumetric strain $\epsilon_v$ and the deviatoric strain $\epsilon_q$. Stress invariants have already been defined above for total stresses. The same definition is valid for effective stresses. The soil mechanics sign convention is adopted, in which the plus sign denotes compression. The strain invariants are defined as follows:

$$\epsilon_v = \epsilon_1 + 2\epsilon_3, \tag{1}$$

$$\epsilon_q = \frac{2}{3}(\epsilon_1 - \epsilon_3), \tag{2}$$

where $\epsilon_1$ and $\epsilon_3$ denote vertical and horizontal strains, respectively.

**4.2. Isotropic compression.** Figure 5 shows the stress-strain curves obtained from isotropic compression tests (path 0A0). The shape of these curves is similar for both initially loose and dense sands (or initially contractive and dilative sands). Note that the deviatoric strains were recorded during isotropic compression, which means that the specimens were not ideally isotropic. This phenomenon has also been observed by other researchers, but is generally ignored in modeling as insignificant, see [15].

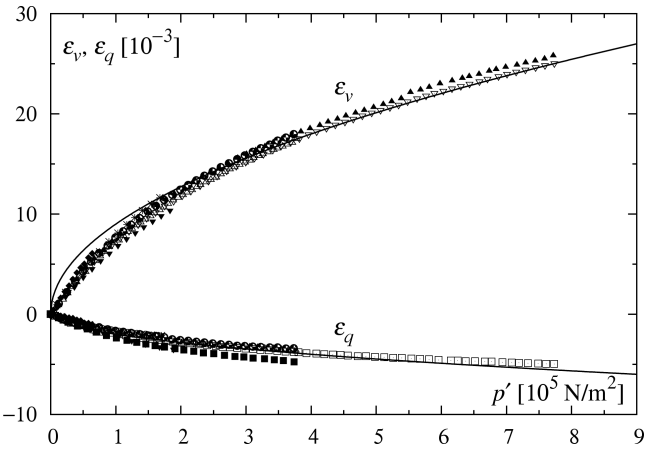


Fig. 5. Stress-strain curves for the isotropic compression of the "Gdynia" sand

The curves shown in Fig. 5 can be approximated by analytical formulae, which is a matter of convenience. For example, the following formulae can be applied:

$$\epsilon_v = A_v \sqrt{p'} \tag{3}$$

$$\epsilon_q = A_q \sqrt{p'}, \tag{4}$$

where $A_v$ and $A_q$ are certain coefficients, the values of which are different for loading and unloading.

It is also convenient, for practical reasons, to introduce the **stress unit** $10^5$ N/m$^2$ and the **strain unit** $10^{-3}$, as shown in Fig. 5. Thus, if $p' = 200$ kPa = $2 \times 10^5$ N/m$^2$, only 2 is introduced into Eqs. (3) and (4). If, for example, one obtains $\epsilon_v = 3$ from Eq. (3), it should be remembered that $\epsilon_v$ is expressed in the above unit, i.e. $\epsilon_v = 3 \times 10^{-3}$. An advantage of using these units is that the stresses and strains are of the same order of magnitude, which is convenient in algebraic manipulations. For the curves shown in Fig. 5, one obtains the following values of the coefficients for loading: $A_v = 9$, $A_q = -2$.

The values of the above coefficients depend on the initial relative density of sand. For example, Sawicki and Świdziński [16] have shown that for another model sand ("Skarpa"), the values of $A_v$ are in the range of 3.7–7.3 for an initially loose sand ($0.016 \leq I_D \leq 0.445$), and in the range of 2.2–4.5 for an initially dense sand ($0.71 \leq I_D \leq 0.86$), with the

average values of 6 and 3.5, respectively. The average values of $A_q$ were $-0.95$ and $-0.53$ respectively for initially loose and dense specimens.

**4.3. Pure shearing.** Figure 6 shows deviatoric strains that develop during the pure shearing (path ABC) of an initially contractive sand, as a single, common plot for three experimental curves corresponding to different values of the mean effective stress. The plot is presented in terms of new variables: $\epsilon_q/\sqrt{p'}$ and $\eta = q/p'$. The following analytical approximation of this plot is convenient:

$$\frac{\epsilon_q}{\sqrt{p'}} = \frac{c\eta}{\eta'' - \eta}, \tag{5}$$

where $c$ is a coefficient, and $\eta''$ corresponds to the critical/steady state. Usually this condition is identified with the Coulomb-Mohr criterion. Therefore:

$$\eta'' = 6\sin\phi/(3 - \sin\phi), \tag{6}$$

where $\phi$ is the angle of internal friction.

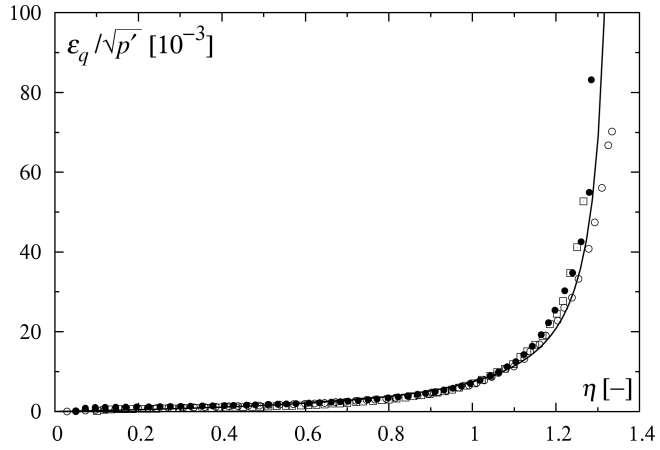


Fig. 6. Deviatoric strains that develop during pure shearing (path ABC in Fig. 4) – a common plot for three experiments performed at different values of the mean effective stress

The shape of the plot shown in Fig. 6 is similar for initially loose and dense specimens, or initially contractive and dilative specimens. The following values of parameters were determined for an initially loose "Gdynia" sand: $c = 2.6$, $\eta'' = 1.35$ and for an initially dense sand: $c = 1.2$, $\eta'' = 1.55$.

Figure 7 shows a single, common plot for volumetric strains that develop during the pure shearing of an initially contractive "Gdynia" sand. The shape of this function can be approximated by the following expression:

$$\frac{\epsilon_v}{\sqrt{p'}} = c_1\eta^4, \tag{7}$$

where $c_1 = 3$.

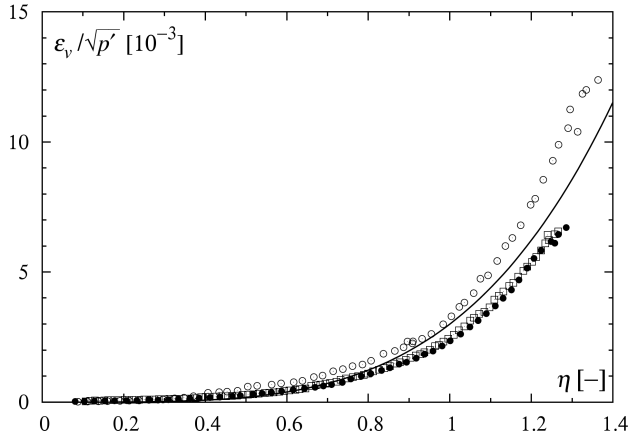


Fig. 7. Volumetric strains during the shearing of an initially contractive "Gdynia" sand – a common plot

Recall that at the critical/steady state, the plastic flow takes place at a constant volume. This means that the maximum value of compaction during shearing can be determined from the state parameter $s$, which is defined as a distance from the initial point on the plot $\log p', e$ (say point A in Fig. 2) to SSL [15]. Consequently, there should be $c_1 = c_1(s)$. This also means that there is no single material constant characterizing volumetric changes during the shearing of an initially contractive sand, but rather a function of a given shape, the maximum value of which depends on the state parameter.

Figure 8 shows a single, common plot for volumetric strains that develop during the shearing of an initially dilative sand (path CD in Fig. 2). During the first stage of shearing, the sand compacts, and after reaching $\eta = \eta'$ the process of dilation begins. Since it is difficult to approximate the plot shown in Fig. 8 by a single analytical expression, it was approximated by the two following functions:

$$\frac{\epsilon_v}{\sqrt{p'}} = a_1\eta^2 + a_2\eta, \quad 0 \le \eta \le \eta', \tag{8}$$

$$\frac{\epsilon_v}{\sqrt{p'}} = (a_3\eta + a_4)\exp(a_5\eta), \quad \eta' \le \eta \le \eta'', \tag{9}$$

where $a_1 = -0.5$, $a_2 = 1$, $a_3 = -0.0716$, $a_4 = 0.0897$, $a_5 = 3.3$.

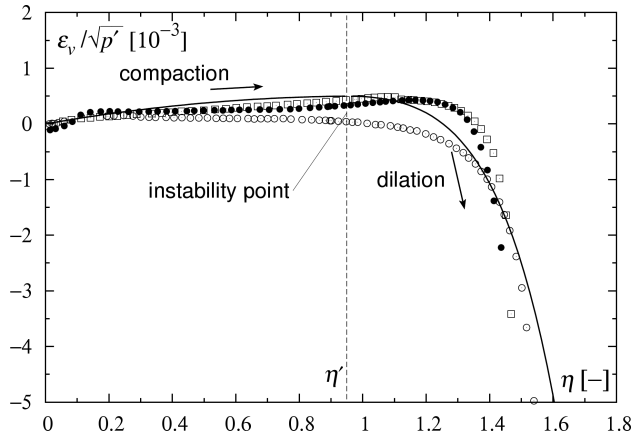


Fig. 8. Volumetric strains during the shearing of an initially dilative "Gdynia" sand – a common plot

Note that the functions (8) and (9) are continuous at $\eta = \eta'$ and have a continuous first derivative. Recall that Eqs. (5), (7), (8) and (9) approximate the strains that develop during loading, i.e. when $\mathrm{d}\eta > 0$ or $\mathrm{d}q > 0$.

### 4.4. Some remarks.

- The above experiments provide a picture of the pre-failure behaviour of dry or fully drained sand subjected to isotropic compression and to pure shearing. Such a distinction of two basic types of loading follows from the classical decomposition of stress and strain tensors into spherical and deviatoric parts. Each of these parts is responsible for characteristic phenomena observed in granular soils. Note that the role of the spherical part of the stress tensor is "constructive", since the soil skeleton becomes stronger as the mean effective stress increases. The role of the stress deviator is "destructive", since it is responsible for a progressive weakening of sand and its failure.
- The presentation of experimental results in an analytical form and in the form of common plots facilitates the analysis of experimental data. It also makes it possible to construct new theoretical models of sand and to validate the existing models. For example, on the basis of such results obtained for another model soil ("Skarpa"), Sawicki and Świdziński [16] have proposed a simple incremental model describing the pre-failure behaviour of sands. That model leads to predictions of the pre-failure behaviour of granular soils, both drained and undrained, which are conformable with experimental data, see [17]. It also makes it possible to study various instabilities that are experimentally observed in sands, cf. [18].
- An important aspect of the experiments proposed is that the initial state of sand, defined as either contractive or dilative, was taken into account. Figures 7 and 8 show the basic difference between the behaviour of sand, being in either contractive or dilative initial states. The behaviour of an initially dilative sand is peculiar, as it first compacts and then strongly dilates. The non-dimensional stress $\eta = \eta'$, corresponding to this change, can be identified with the instability line, which is a relatively novel geometrical object, only recently introduced into soil mechanics, see [19–22]. The relation between $\eta'$ and the instability line has not been discovered before, although many plots, similar to that in Fig. 8, have been published.
- It will be shown later how to determine the instability line from other experiments. For example, the experiments under undrained conditions, performed on initially contractive sands, lead to the so-called static liquefaction. The maximum shear stress that can be supported by the soil skeleton in this special case can be identified with the instability line.

## 5. Oedometric behaviour

The oedometer is a simple geotechnical device used for collecting basic data under specific conditions in which the horizontal displacements of the soil are prevented by rigid walls. Such conditions often occur in real-life geotechnical situations, and that is why such experiments are very important. Most geotechnical apparatuses are not equipped with gauges for the measurement of lateral stresses which develop during such experiments, so they provide only limited information about soil behaviour.

Note that the oedometric conditions can also be simulated in triaxial apparatuses equipped with gauges measuring lateral strains. However, such experiments are rather complicated, as the stress path corresponding to these conditions should be incrementally adjusted to the general condition $\epsilon_3 = 0$. Oedometric experiments can serve as a kind of verification of the corresponding triaxial investigations, and they are also a basis for the determination of basic mechanical properties of soils.

**5.1. Basic experimental data.** The experiments were performed in an oedometer capable of measuring lateral stresses (Fig. 9, see [23]). The vertical stress $\sigma_z$ was incrementally applied and the vertical displacement was measured directly. The lateral stress $\sigma_x$ was measured indirectly with a strain gauge installed on the cylindrical wall of the oedometer. The basic set of experiments included a few (usually 3–5) cycles of loading and unloading. Typical experimental records, corresponding to the "Gdynia" sand, are shown in Figs. 10 and 11. Figure 10 illustrates the relation between the vertical stress and vertical strain, and Fig. 11 shows the relation between vertical and lateral stresses. These relations correspond to an initially loose sand, characterized by $I_D = 0.217$.

Fig. 9. An oedometer for the measurement of lateral stresses, constructed at IBW PAN

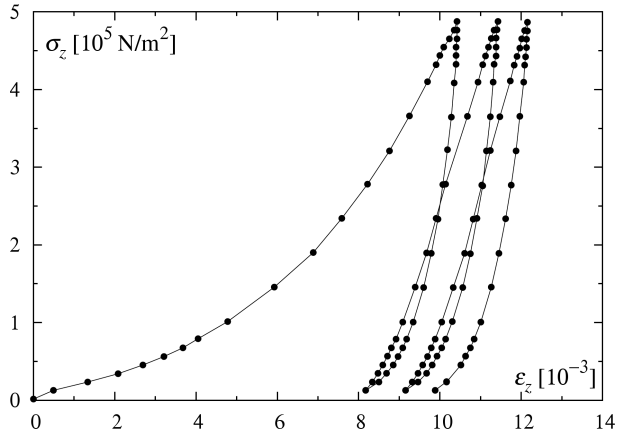


Fig. 10. Vertical stress-strain curves in oedometric conditions for the "Gdynia" sand

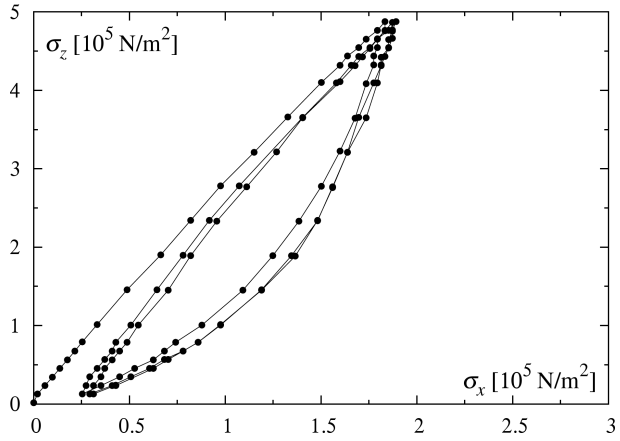


Fig. 11. Vertical-lateral stress curves in oedometric conditions for the "Gdynia" sand

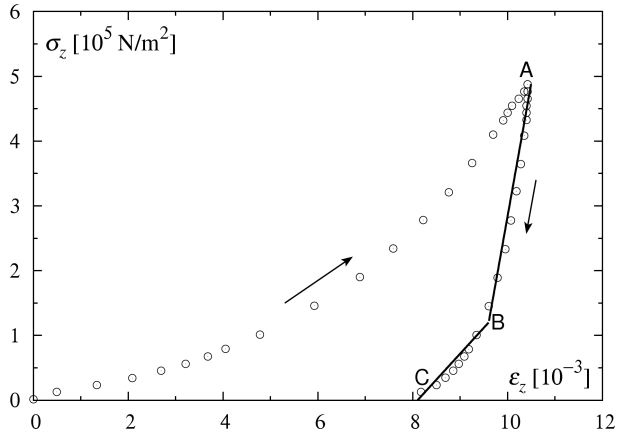


Fig. 12. A bilinear approximation of oedometric unloading, cf. Fig. 10

**5.2. Interpretation of experimental data.** Experimental results, summarized in Figs. 10 and 11, are the basis for determining various mechanical properties of sand, including standard geotechnical interpretations. For example, for the virgin loading (first cycle) shown in Fig. 10, one can find the following analytical approximation of the vertical stress-strain curve:

$$\sigma_z = A\epsilon_z^2, \tag{10}$$

where $A = 0.045$. Recall respective units.

The loading parts of the stress paths shown in Fig. 11 make it possible to determine the coefficient $K_0$, which in the case considered is equal to 0.37. Recall that $\sigma_x = K_0\sigma_z$.

The unloading parts of the curves shown in Figs. 10 and 11 can also be used to estimate the elastic moduli of sand, assuming a bilinear approximation of these curves [23]. Such an approximation is shown for the data presented in Figs. 10 and 11. The first sector of unloading, AB, represents the elastic response of sand which follows from the analysis of corresponding sectors in subsequent cycles. The slopes of these sectors are the same as the slope of the AB sector in the first cycle.

Experimental data shown in Figs. 12 and 13 suggest that the first part of unloading can be approximated by a model of linear elasticity. The elastic modulus $E$ and Poisson's ratio $\nu$ are given by the following formulae:

$$E = E^* \left[1 - \frac{2}{a(1+a)}\right], \tag{11}$$

$$\nu = \frac{1}{1+a} \tag{12}$$

where $E^*$ and $a$ denote the slopes of the AB sectors in Figs. 12 and 13, i.e.

$$E^* = \frac{\sigma_z^A - \sigma_z^B}{\epsilon_z^A - \epsilon_z^B}, \tag{13}$$

$$a = \frac{\sigma_z^A - \sigma_z^B}{\sigma_x^A - \sigma_x^B}. \tag{14}$$

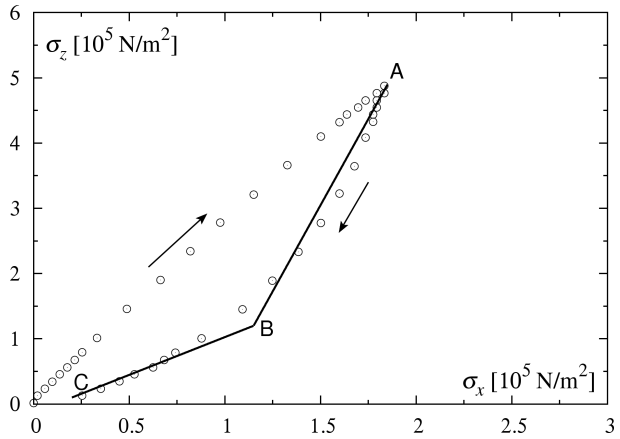


Fig. 13. A bilinear approximation of unloading, cf. Fig. 11

For the data corresponding to Figs. 12 and 13 one obtains the following values of these moduli: $E = 2.85$ ($\times 10^8$ N/m$^2$) and $\nu = 0.16$. Experimental results obtained from the oedometric tests with additional measurements of lateral stresses can also be used for other interpretations of the mechanical behaviour of sand, for example, an elasto-plastic interpretation [24].

## 6. Cyclic loading properties

**6.1. Simple cyclic shearing.** Cyclic loading soil mechanics has been developed for half a century, and there already exists an extensive literature on this subject, including [15, 25, 26], to mention but a few sources, in which hundreds of further references can be found. Cyclic loadings cause the densification of dry or fully drained sand, and under undrained conditions, they lead to pore-pressure generation and subsequent liquefaction.

The cyclic loading properties of sands have been investigated experimentally mainly in triaxial apparatuses, but also in some other devices, such as the simple cyclic shearing apparatus, the oedometer or the cyclic hollow cylinder apparatus. In this section, some very basic experiments performed on dry sand in a simple shearing apparatus will be described. Figure 14 shows the basic idea of such a device, which has

been constructed at the Institute of Hydro-Engineering, see also Fig. 15.

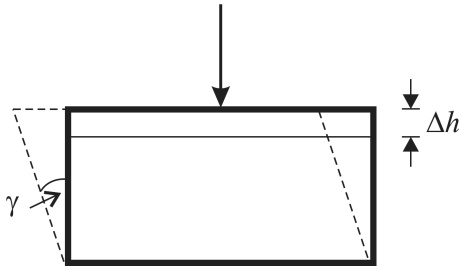


Fig. 14. The basic idea of a cyclic simple shear apparatus

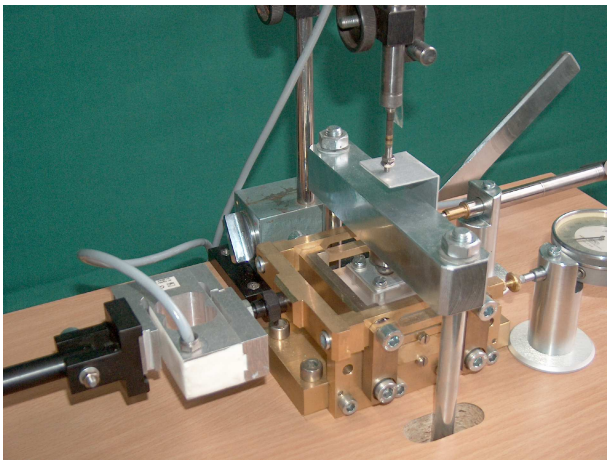

Fig. 15. A cyclic simple shear apparatus constructed at IBW PAN

A rectangular parallelepiped sand specimen is subjected to cyclic shearing at a given cyclic shear strain amplitude $\gamma_0$. A vertical force (stress) is applied to the rectangular plate that is placed on the top surface of the specimen. The vertical displacement of this plate is measured as a function of the number of loading cycles $N$. The aim of this simple experiment is to obtain compaction (densification) curves as functions of cyclic shear strain amplitudes and the number of loading cycles.

**6.2. Typical experimental results.** Figure 16 shows typical experimental records, where the volumetric strain $\epsilon_v$ is plotted against the number of loading cycles $N$, treated as a continuous variable, and for different values of cyclic shear strain amplitudes. These results support some original findings that the cyclic loading compaction of dry sand depends on the cyclic shear strain amplitude and the number of loading cycles, see [27]. It was also found that the compaction does not depend on the mean effective stress (i.e. vertical stress), nor on the frequency of cyclic loading.

The experimental results shown in Fig. 16 can be plotted in the form of a single, common compaction curve if the following new variables are introduced:

$$z = \gamma_0^2 N/4, \tag{15}$$

$$\Phi = \frac{1-n_0}{n_0}\epsilon_v, \tag{16}$$

where $n_0$ denotes the initial porosity.

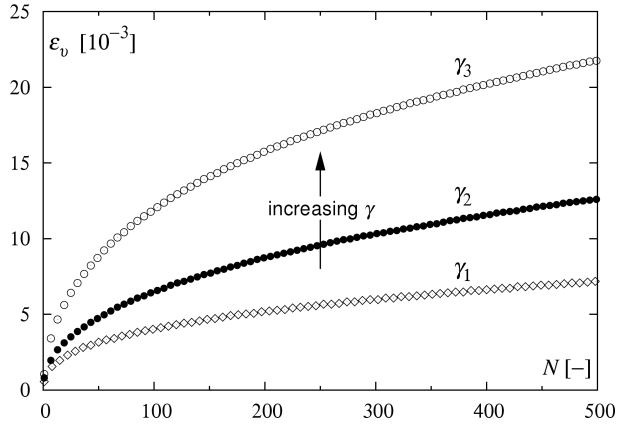


Fig. 16. Compaction curves as functions of the cyclic shear strain amplitude and the number of loading cycles

Figure 17 shows the plot $\Phi = \Phi(z)$ in which the three distinct curves from Fig. 16 form a common (or universal) compaction curve. An analytical approximation of this curve is the following:

$$\Phi = C_1 \ln(1 + C_2 z), \tag{17}$$

where $C_1 = 9.08$ and $C_2 = 0.055$ for the "Gdynia" sand (recall respective units). Such a curve can be a basis for theoretical investigations aimed at establishing respective constitutive relations, cf. [28].

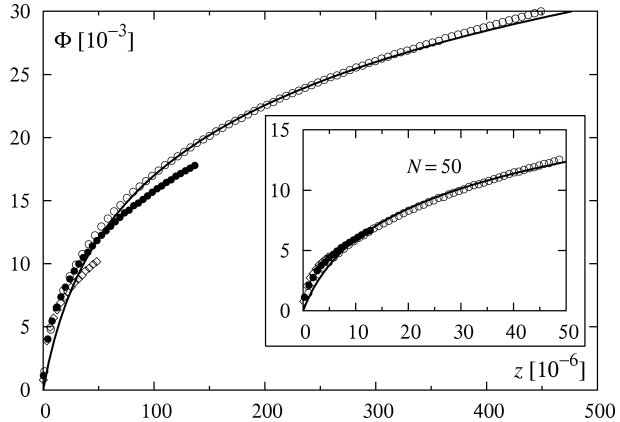


Fig. 17. A common compaction curve for the data from Fig. 16

The common compaction curve shown in Fig. 17 is a good approximation of experimental data for a relatively small number of loading cycles, say $N < 100$. For a larger number of loading cycles, up to the order of $10^5$, other approximations are necessary, see [29, 30]. However, the formula (17) is very useful in many applications, including earthquake geotechnics, see [31].

## 7. Experimental determination of the instability line

It is a common practice in soil mechanics to use various geometrical objects that help in the analytical studies of empirical results, such as yield surfaces etc. One of such characteristic objects is the instability line, defined in the effective stress space for the triaxial configuration. It was already shown (cf. Fig. 8 and remarks in Sec. 4), that the instability line can be determined from the pure shearing of an initially dilative sand. This line can also be determined from other experiments, which will be briefly described, see [17, 18].

**7.1. Spherical unloading.** Figure 18 illustrates the basic idea of an unstable behaviour of an initially contractive sand during a spherical unloading of the "Gdynia" sand, investigated in a triaxial apparatus. The specimens should be dry or water saturated, but under fully drained conditions. First, a specimen is isotropically loaded (path 0a) and then sheared at a constant mean stress (path ab). Then, the spherical unloading (path bcd) at a constant deviatoric stress takes place. A characteristic feature of the sand behaviour during the spherical unloading is that it first dilates (path bc) and then suddenly compacts (path cd). The point c corresponds to the instability line. Similar experiments should be performed for a few values of a constant deviatoric stress.

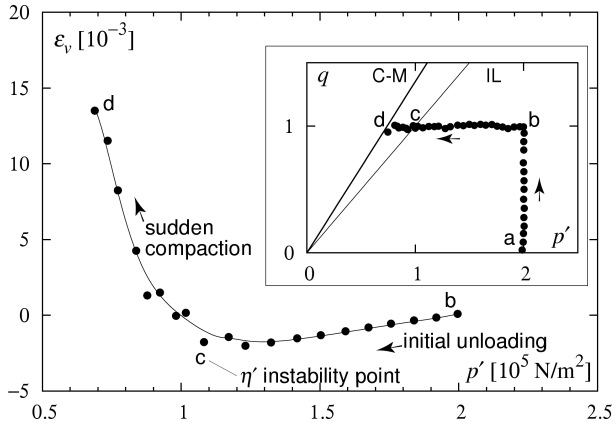


Fig. 18. The instability of an initially contractive "Gdynia" sand during spherical unloading

**7.2. Static liquefaction.** Another interesting, and well-known, experiment deals with the shearing of an initially contractive saturated specimen under undrained conditions. Firstly, the specimen is isotropically pre-loaded (path 0a in Fig. 19) with the initial pore-pressure $u = 0$. Then, the cell pressure is kept constant, and the deviatoric stress increases. During the experiment the pore-pressure increases (it should be measured), and the mean effective stress decreases. The maximum value of the deviatoric stress is reached at the instability line. After reaching this line, the deviatoric stress suddenly drops and the phenomenon of static liquefaction takes place.

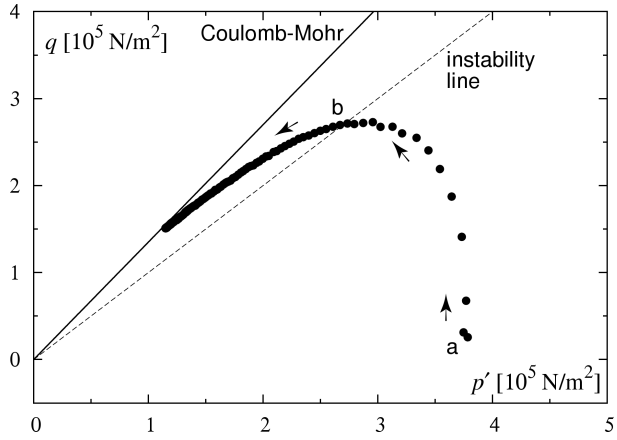


Fig. 19. The static liquefaction of an initially contractive "Gdynia" sand

## 8. Discussion

1. A set of experiments that make it possible to determine basic mechanical properties of granular soils is proposed. Subjective as it may look, this set of experiments collates some basic findings of contemporary soil mechanics. The proposed experiments make it possible to determine the initial state of soil, its pre-failure behaviour, including some instabilities, up to the limit/steady state.
2. The results of the proposed experiments make it possible to formulate or calibrate partial models of soil behaviour. Such an approach, that is, the formulation of partial models, may well be the only way to deal with extremely complicated problems of soil mechanics, at least at the present state of knowledge. Soil mechanics still needs its own Newton to formulate a unified theory.
3. Admittedly, the experiments proposed require equipment that is above average geotechnical standards, and they are also rather laborious, which makes them expensive. It is our task to reduce these costs and to make the basic geotechnical investigations as simple as possible.
4. The experimental results presented in this paper have served to formulate various models of the behaviour of granular soils. They may also serve as a basis for the validation of other models, particularly as these experiments were performed on a single model sand "Gdynia".

**Acknowledgements.** Research presented in this paper was supported by the Polish Ministry of Science and Higher Education (project N N 506 072938). We appreciate this support.

REFERENCES

[1] M. Bolton, *Micro-geomechanics, Lecture Notes*, University of Cambridge, Cambridge, 2001.
[2] D. Kolymbas, "The misery of constitutive modelling", in: *Constitutive Modelling of Granular Materials*, ed. D. Kolymbas, pp. 11–24, Springer, Berlin, 2000.
[3] W.F. Chen, *Limit Analysis and Soil Plasticity*, Elsevier, Amsterdam, 1975.

[4] W. Derski, R. Izbicki, I. Kisiel, and Z. Mróz, *Rock and Soil Mechanics*, ed. I. Kisiel, PWN, Warsaw, 1982 (in Polish).
[5] A. Saada and G. Bianchini, *Constitutive Equations for Granular Non-Cohesive Soils*, Balkema, Rotterdam, 1989.
[6] B.K. Menzies, "A computer controlled hydraulic triaxial testing system", in: *Advanced Triaxial Testing of Soil and Rock, ASTM STP 977*, eds. R.T. Donaghe, R.C. Chaney and M.L. Silver, pp. 82–94, ASTM, Philadelphia, 1988.
[7] R.F. Craig, *Soil Mechanics*, Van Nostrand Reinhold, Wokingham, Berkshire, 1987.
[8] G. Castro, "Liquefaction and cyclic mobility of saturated sands", *J. Geotechnical Eng., ASCE* 101 (GT6), 551–569 (1975).
[9] S.J. Poulos, "The steady state of deformation", *J. Geotechnical Eng., ASCE* 107 (GT5), 501–516 (1981).
[10] K. Been and M.G. Jefferies, "A state parameter for sands", *Geotechnique* 35 (2), 99–112 (1985).
[11] K. Been, M.G. Jefferies, and J. Hachey, "The critical states of sands", *Geotechnique* 41 (3), 365–381 (1991).
[12] J. Chu and K.W. Leong, "Pre-failure strain softening and pre-failure instability of sands: a comparative study", *Geotechnique* 51 (4), 311–321 (2001).
[13] Z. Wiłun, *Outlines of Geotechnics*, WKiŁ, Warsaw, 2010 (in Polish).
[14] J. Tejchman, *Finite Element Modeling of Shear Localization in Granular Bodies in Hypoplasticity with Enhancements*, Gdańsk Univeristy of Technology Publishers, Gdańsk, 2005.
[15] M. Jefferies and K. Been, *Soil Liquefaction: A Critical State Approach*, Taylor and Francis, London, 2006.
[16] A. Sawicki and W. Świdziński, "Stress-strain relations for dry and saturated sands, Part I: Incremental model", *J. Theoretical and Applied Mechanics* 48 (2), 309–328 (2010a).
[17] A. Sawicki and W. Świdziński, "Stress-strain relations for dry and saturated sands, Part II: Predictions", *J. Theoretical and Applied Mechanics* 48 (2), 329–373 (2010b).
[18] A. Sawicki and W. Świdziński, "Modelling the pre-failure instabilities of sand", *Computers and Geotechnics* 37(6), 781–788 (2010c), [doi: 10.1016/j.compgeo.2010.06.004].
[19] J.M. Konrad, "Undrained response of loosely compacted sands during monotonic and cyclic compression tests", *Geotechnique* 43 (1), 69–89 (1993).
[20] P.V. Lade, "Static instability and liquefaction of loose fine sandy slopes", *J. Geotechnical Eng., ASCE* 118 (1), 51–71 (1992).
[21] P.V. Lade, "Instability of granular materials", in: *Physics and Mechanics of Soil Liquefaction*, eds. P.V. Lade and J.A. Yamamuro, pp. 3–16, Balkema, Rotterdam, 1999.
[22] P.V. Lade, R.B. Nelson, and Y.M. Ito, "Nonassociated flow and stability of granular materials", *J. Engineering Mechanics, ASCE* 113 (9), 1302–1318 (1987).
[23] A. Sawicki and W. Świdziński, "Elastic moduli of non-cohesive particulate materials", *Powder Technology* 96, 24–32 (1998).
[24] A. Sawicki, "Elasto-plastic interpretation of oedometric tests", *Archives of Hydro-Engineering and Environmental Mechanics* 41 (1–2), 111–131 (1994).
[25] K. Ishihara, *Soil Behaviour in Earthquake Geotechnics*, Clarendon Press, Oxford, 1996.
[26] A. Sawicki and J. Mierczyński, "Developments in modeling liquefaction of granular soils, caused by cyclic loads", *Applied Mechanics Reviews, Trans. ASME* 59 (2), 91–106 (2006), [doi:10.1115/1.2130362].
[27] M.L. Silver and H.B. Seed, "Volume changes in sands during cyclic loading", *J. Soil Mech. Foundation Div., ASCE* 97 (SM9), 1171–1182 (1971).
[28] A. Sawicki, "An engineering model for compaction of sand under cyclic loading", *Engineering Transactions* 35 (4), 677–693 (1987).
[29] T. Wichtmann, A. Niemunis, and Th. Triantafyllidis, "Strain accumulation in sand due to cyclic loading: drained triaxial tests", *Soil Dynamics and Earthquake Engineering* 25, 967–979 (2005).
[30] A. Sawicki, J. Mierczyński, and W. Świdziński, "Strains in sand due to cyclic loading in triaxial conditions", *Archives of Hydro-Engineering and Environmental Mechanics* 56 (1–2), 63–98 (2009).
[31] A. Sawicki and W. Świdziński, "A study on liquefaction susceptibility of some soils from the coast of Marmara sea", *Bull. Pol. Ac.: Tech.* 54 (4), 405–418 (2006).